JOURNAL OF THERMOPHYSICS AND HEAT TRANSFER
Vol. 16, No. 1, January–March 2002

Fractal Models for the Effective Thermal Conductivity of Bidispersed Porous Media

Boming Yu* and Ping Cheng†
Hong Kong University of Science and Technology, Clear Water Bay, Kowloon, Hong Kong, People's Republic of China

Two fractal models for determination of the effective thermal conductivity of bidispersed porous media are developed based on the fractal theory and electrical analogy technique. The theoretical predictions from the proposed fractal thermal conductivity models are compared with those from the previous lumped-parameter model and from experimental data. The results from the proposed fractal models are shown to be in good agreement with both the lumped-parameter model and the experimental data.

Nomenclature

A = area of the cross section of a representative cell
a = size or diameter
D_f = fractal dimension
D_T = tortuosity fractal dimension
d = characteristic diameter of a cluster
d_0 = the minimum diameter of a particle
k = thermal conductivity
L = length scale
L_t = total length due to tortuosity
L_0 = representative length
N = number
R = resistance
r = radium of a cluster
V = volume fraction
β = ratio of thermal conductivity, k_s/k_f
γ_a = ratio of geometrical length scale for a cluster, l_c/a_c, see Fig. 2a
γ'_a = ratio of geometrical length scale for a cluster, a_c/λ, see Fig. 2a
γ_{a1} = ratio of geometrical length scale for a particle, l/a, see Fig. 2b
γ'_{a1} = ratio of geometrical length scale for a particle, a/λ, see Fig. 2b
γ_c = ratio of contact length scale for a cluster, c_c/l_c, see Fig. 2a
γ_{c1} = ratio of contact length scale for a particle, c/l, see Fig. 2b
λ = diameter
ϕ = averaged porosity of a bidispersed porous medium

Subscripts

c = clusters
e = effective
f = fluid
max = maximum
mc = mixed chains of particles or clusters with fluid
min = minimum
n = nontouching particles or clusters
s = solid
t = total
1 = particle

Superscript

$+$ = dimensionless

Received 19 October 2000; revision received 25 May 2001; accepted for publication 10 July 2001.

*Professor, Department of Mechanical Engineering; currently Professor, Department of Physics, Huazhong University of Science and Technology, 1037 Luoyu Road, Wuhan 430074, People's Republic of China; yu3838@public.wh.hb.cn.

†Professor, Department of Mechanical Engineering. Associate Fellow AIAA.

I. Introduction

THE effective thermal conductivities of porous media, such as packed beds, granular materials, fibrous composites, dispersed spheres, and so on, have received much attention[1–8] in the past three decades due to their importance in engineering problems. It is known that heat conduction through saturated porous media strongly depends on the thermal conductivities of the solid and the fluid phase, the shape and distribution of the solid phase, as well as the size of the contact areas between solid particles. To analyze the thermal conductivity of a porous medium, it is usually assumed that the medium has a periodic structure, and a unit cell or representative cell is often chosen for such a study. Based on this approach, Hsu et al.[6] and Cheng and Hsu[7] developed a lumped-parameter model to determine the effective stagnant thermal conductivity of two-dimensional and three-dimensional monodispersed porous media with periodic structures. The methods and models used for the determination of thermal conductivity of monodispersed porous media have recently been reviewed by Cheng and Hsu.[7]

Most recently, a great deal of attention has been given to study the bidispersed porous media that have been used as wicks in heat pipes. The bidispersed porous structure, as shown in Fig. 1a, is composed of clusters that are agglomerated by small particles. In this bidispersed porous medium, there are micropores and macropores within and between the clusters of particles, respectively. Figure 1b is an image of the bidispersed porous medium at magnification of 50. In Fig. 1b, the clusters are in white and the pores are in black, which show that they have disordered structures. Chen et al.[8] analyzed the thermal conductivity of a bidispersed porous medium by assuming that the medium in the microlevel (within the cluster) and in the macrolevel (between clusters) consists of spatially periodic porous cubes, both of which were modeled as three-dimensional touching cubes. They applied the lumped-parameter model[6] to obtain the following expression for the dimensionless effective thermal conductivity of the bidispersed porous medium:

$$k_e^+ = 1 - \gamma_a^2 - 2\gamma_a\gamma_c + 2\gamma_a^2\gamma_c + \frac{\gamma_a^2\gamma_c^2}{1/k_{e,c}^+} + \frac{\gamma_a^2 - \gamma_a^2\gamma_c^2}{1 - \gamma_a + \gamma_a/k_{e,c}^+} + \frac{2(\gamma_a\gamma_c - \gamma_a^2\gamma_c)}{1 - \gamma_a\gamma_c + \gamma_a\lambda_c/k_{e,c}^+} \tag{1}$$

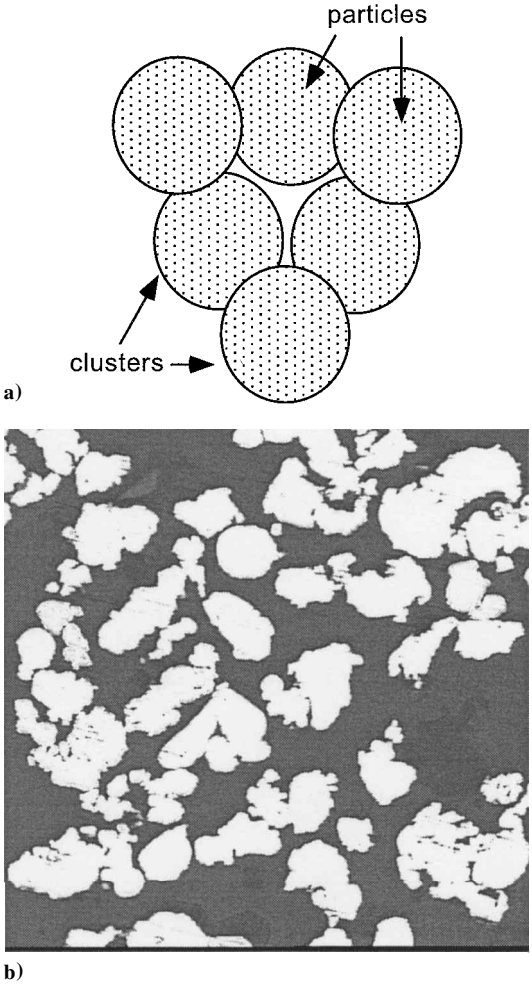

Fig. 1 Top view of a bidispersed medium: a) schematic of the bidispersed porous medium and b) image photograph of the bidispersed porous medium at magnification of 50, white are solid clusters and the black are pores (or fluid).

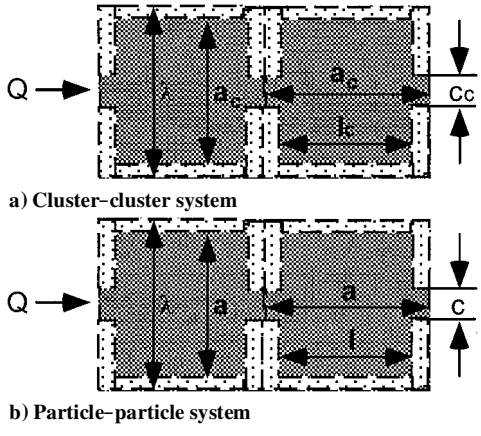

Fig. 2 Unit cell for the lumped parameter method[8]: ●, particles or clusters and ▨, fluid.

with $\gamma_a = l_c/a_c$ and $\gamma_c = c_c/l_c$, where ℓ_c and a_c are the geometric lengths, and c_c is the contact length of the clusters (at the macroscale level) (see Fig 2a). The quantity $k^+_{e,c}$ in Eq. (1) is the dimensionless thermal conductivity of the particles (at the microscale level), which is given by

$$k^+_{e,c} = 1 - \gamma^2_{a1} - 2\gamma_{a1}\gamma_{c1} + 2\gamma^2_{a1}\gamma_{c1} + \frac{\gamma^2_{a1}\gamma^2_{c1}}{1/\beta} + \frac{\gamma^2_{a1} - \gamma^2_{a1}\gamma^2_{c1}}{1 - \gamma_{a1} + \gamma_{a1}/\beta} + \frac{2\left(\gamma_{a1}\gamma_{c1} - \gamma^2_{a1}\gamma_{c1}\right)}{1 - \gamma_{a1}\gamma_{c1} + \gamma_{a1}\lambda_{c1}/\beta} \tag{2}$$

where $\beta = k_s/k_f$ is the ratio of thermal conductivity, $\gamma_{a1} = l/a$ is the ratio of geometrical length scale for a particle, and $\gamma_{c1} = c/l$ is the ratio of contact l ength scale for a particle (see Fig. 2b). The total porosity of the bidispersed porous media is given by

$$\phi = 1 - \left[\left(1 - 3\gamma^2_c\right)\gamma^3_a + 3\gamma^2_c\gamma^2_a\right](1 - \phi_c) \tag{3}$$

where ϕ_c is the porosity within the microporous cubes (clusters), which is given by

$$\phi_c = 1 - \left(1 - 3\gamma^2_{c1}\right)\gamma^3_{a1} - 3\gamma^2_{c1}\gamma^2_{a1} \tag{4}$$

Chen et al.[8] found that the predicted thermal conductivity from Eqs. (1–4) is in good agreement with their experimental measurements.

The disordered nature of the micropores inside the clusters and macropores between clusters in bidispersed porous media suggests that the fractal theory[9–15] may be used to predict properties of a bidispersed porous medium. In a recent paper, Yu and Cheng[15] developed a fractal permeability model for bidispersed porous media and found that their model predictions are in good agreement with experimental data.

In this work, we focus our attention on developing a fractal model for the effective thermal conductivity of the bidispersed porous media. The proposed fractal models are compared with both the lumped-parameter model and experimental data. This paper is organized as follows. Section II provides a brief introduction of the fractal theory, which is the basis of the present model. Section III introduces the fractal description of the microstructures of the bidispersed porous media based on which a fractal thermal conductivity model is derived in Sec. IV. The results and discussion are given in Sec. V. Section VI summarizes the findings of this work.

II. Basic Fractal Theory

Euclidean geometry describes ordered objects such as points, curves, surfaces, and cubes using integer dimensions 0, 1, 2, and 3, respectively. Associated with each dimension is a measure of the object such as the length of a line, the area of a surface, and the volume of a cube. The measures are invariant with respect to the unit of measurement used. However, numerous objects found in nature,[9] such as rough surfaces, coast lines, mountains, rivers, lakes, and islands, are disordered and irregular, and they do not follow the Euclidean description due to the scale-dependent measures of length, area, and volume. These objects are called fractals, and the dimensions of such objects are nonintegral, which are defined as fractal dimensions.[9,10] The measure of a fractal object, $M(L)$, is related to the length scale L through a scaling law in the form of

$$M(L) \sim L^{D_f} \tag{5}$$

where M can be the length of a line, the area of a surface, the volume of a cube, or the mass of an object, and D_f is the fractal dimension of an object. Equation (5) implies the property of self-similarity, which means that the value of D_f from Eq. (5) keeps constant over a range of length scales L. The geometry structures such as Sierpinski gasket, Sierpinski carpet, and Koch curve are the examples of the exact self-similar fractals, which exhibit the self-similarity over an infinite range of length scales.[9,10] However, the exactly self-similar fractals in a global sense are rarely found in nature. Many objects found in nature (such as the coast lines of islands) are not exactly self-similar, they are statistically self-similar. These objects exhibit the self-similarity in some average sense and over a certain local range of length scales L. The fractal dimension D_f used in this paper is referred to both the statistical and the exact fractals.

III. Fractal Characterization of Microstructures of the Bidispersed Porous Media

As shown in Fig. 1, a bidispersed porous medium contains many clusters formed by particle agglomeration. There are two types of pores: macropores (on the order of 10^{-3} m) between clusters and micropores (on the order of 10^{-5} m) between particles inside each

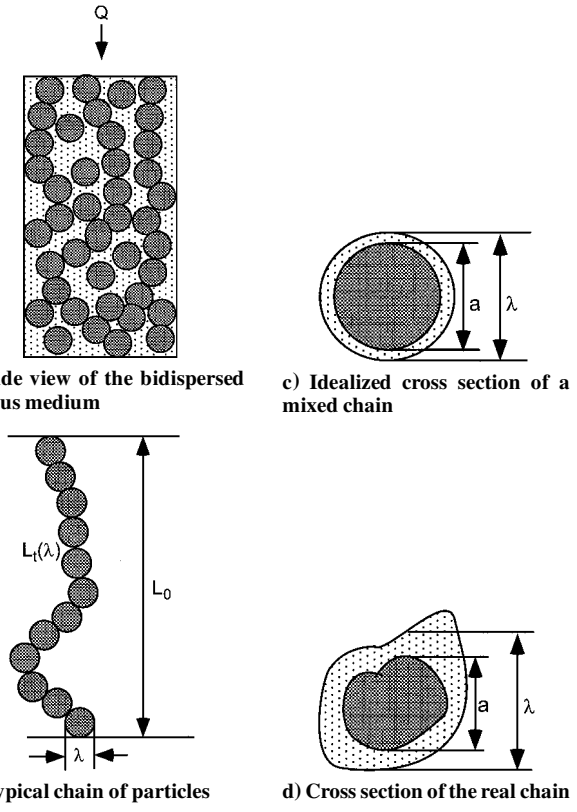

a) Side view of the bidispersed porous medium

c) Idealized cross section of a mixed chain

b) Typical chain of particles

d) Cross section of the real chain

Fig. 3 Proposed fractal model for bidispersed porous media: ●, particles or clusters and □, fluids.

cluster. When a bidispersed porous medium is saturated with a fluid, such as resin or other materials, the fluid fills both the micro- and macropores. Both types of pores form irregular and tortuous pore channels, which are called capillaries.

We now apply a fractal analysis based on the unit cell concept to study the thermal conductivity of bidispersed porous media. As shown in Fig. 3a, some particles and clusters contact each other to form irregular and tortuous chains, and others do not touch each other. These irregular and tortuous pore channels (capillaries) and particle and cluster chains are very similar to coast lines. Thus, they exhibit the fractal behavior given by

$$L_t(\lambda)/L_0 = (L_0/\lambda)^{D_T - 1} \tag{6}$$

where D_T is the tortuosity fractal dimension (with $1 < D_T < 2$) representing the extent of convolutedness of capillary pathways for fluid flow through a porous medium. $D_T = 1$ represents a straight capillary path or a straight chain of particles (or clusters), and a higher value of D_T corresponds to a highly tortuous capillary (or chain). In the limiting case of $D_T = 2$, we have a tortuous line so irregular that it fills an entire plane.[16] Note that Eq. (6) diverges as $\lambda \to 0$, which is one of the properties of fractal lines.[10] In Eq. (6), λ is the size of a capillary or a chain in the medium, and $L_t(\lambda)$ is its tortuous length. Because of the tortuous nature of the capillary or chain, $L_t(\lambda) \geq L_0$, where L_0 is the representative length. Thus, $L_t(\lambda) = L_0$ means a straight capillary or chain (see Fig. 3b).

The tortuosity of a capillary pathway or chain is similar to the triadic Koch teragon (see Ref. 9), which satisfies $L(\varepsilon) = \varepsilon^{1-D}$ [where $L(\varepsilon)$ is the length of the triadic Koch teragon whose sides are of length ε], and this formula is identical with Richardson's empirical law relative to the coast of Britain (see Ref. 9). Equation (6) is also similar to the fractal scaling relationship for analysis of dispersion in a single fractal streamtube.[16] It is also one of the fractal scaling laws characterizing the fractal properties of the bidispersed porous media. Besides the convolutedness of the capillary pathways or chains, the number of capillary pathways or chains with the size of λ is an another important property. The number of capillary pathways or chains should follow the following scaling law:

$$N(L \geq \lambda) = (\lambda_{\max}/\lambda)^{D_f} \tag{7}$$

where D_f, the same fractal dimension[17–19] as defined in Eq. (5), is the area fractal dimension of a cross section normal to the heat (or fluid) flow direction with $1 < D_f < 2$. Equation (7) shows that the number of pores or chains becomes infinite as $\lambda \to 0$, which is one of properties of fractal planes.[9] Equation (7) denotes the scaling relationship of the cumulative pore (or chain) population in a cross section. It is analogous to the cumulative size distribution of islands on the Earth's surface that follows the power law $N(A > a) \sim a^{-D/2}$ (Ref. 9), where N is the total number of islands of area A greater than a, and D is the fractal dimension of the surface. Equation (7) is also identical with the power law relation $N(A \geq a) = (a_{\max}/a)^{D/2}$ describing the contact spots on engineering surfaces.[12]

The number of pores (or chains) of sizes lying between λ and $\lambda + d\lambda$ can be obtained by differentiating Eq. (7) to give

$$-dN = D_f \left[\frac{d(\lambda/\lambda_{\max})}{(\lambda/\lambda_{\max})^{D_f + 1}} \right] \tag{8}$$

The negative sign in Eq. (8) implies that the pore (or chain) number decreases with the increase of pore (or chain) size. Equations (5–8) form the basis of the present fractal thermal conductivity model, which will be derived in the next section.

IV. Fractal Thermal Conductivity Model for Bidispersed Porous Media

Model 1

In this section, a fractal model for thermal conductivity of bidispersed porous media is derived analytically. Figure 3a is a schematic of the bidispersed porous medium. It can be seen from Fig. 3a that in a bidispersed porous medium, some particles (or clusters) contact each other to form chains, whereas others do not touch each other (nontouching). These two configurations of particles (or clusters) in a bidispersed medium should be included in the model. We further assume in this model that heat conduction is one dimensional in the unit cell and that the heat flow lines approximately follow the chains. Figure 3b shows the schematic of a chain of particles (or clusters), with a total length of $L_t(\lambda)$ that is greater than L_0, the representative length. The zigzig shape of a chain is similar to the fractal coast lines or fractal streamtubes, which follow Eq. (6). We refer to a mixed chain, which consists of particles (or clusters) and the fluid enclosing these particles (or clusters). Figure 3c shows an idealized cross section of a chain: a circular particle (or cluster) with annular fluid. However, in reality, the particles (or clusters) may not be circular in shape, as shown in Fig. 3d, and the area and shape of cross section of each mixed chain may be different. We assume that the area distribution of cross section of mixed chains follows the same fractal power law as in Eq. (7). The thermal resistance of the mixed chains and nontouching particles (or clusters) can be considered to be in parallel, which can be expressed as

$$1/R_t = 1/R_n + 1/R_{\text{mc}} \tag{9}$$

The effective thermal conductivity of the system can be obtained by

$$k_e = \frac{1}{R_t}\frac{L_0}{A} = \frac{1}{R_n}\frac{L_0}{A} + \frac{1}{R_{\text{mc}}}\frac{L_0}{A} = \frac{1}{R_n}\frac{L_0}{A_n}\frac{A_n}{A} + \frac{1}{R_{\text{mc}}}\frac{L_0}{A}$$

$$= \frac{A_n}{A}k_{e,n} + \left(1 - \frac{A_n}{A}\right)k_{e,\text{mc}} \tag{10}$$

where A is the total area of a representative cross section and A_n is an equivalent area of a cross section having the same porosity as the nontouching particles or clusters, with $0 \leq A_n/A \leq 1$. For a unit cell consisting of two-dimensional nontouching particles, Hsu et al.[6] obtained the following expression for its thermal conductivity:

$$k_{e,n} = k_f\left(1 - \sqrt{1-\phi}\right) + \frac{k_f\sqrt{1-\phi}}{1 + (1/\beta - 1)\sqrt{1-\phi}} \tag{11}$$

which will be used in connection with the first term at the right-hand side of Eq. (10).

Now we focus our attention on the derivation of the effective thermal conductivity $k_{e,\mathrm{mc}}$, which appears at the second term of the right-hand side of Eq. (10). We assume that the contact resistance between particles is only along the heat flow direction. For this purpose, Fig. 2a is adopted as a simplified model for the mixed chain in the direction perpendicular to the heat flow.

If the cube particle (or cluster) model is assumed and there is no heat conduction in the lateral direction, we obtain the following expression for the resistance of a cube particle:

$$R_1 = \frac{1}{\lambda}\left[\frac{\gamma_{a1}}{k_s\gamma'_{a1} + 2k_f(1-\gamma'_{a1})} + \frac{(1-\gamma_{a1})\gamma'_{a1}}{k_s\gamma_{c1}^2\gamma_{a1}'^2/\gamma_{a1}^2 + k_f\left(1-\gamma_{c1}^2\gamma_{a1}'^2/\gamma_{a1}^2\right)}\right] \tag{12}$$

where $\gamma_{a1} = l/a$, $\gamma'_{a1} = a/\lambda$, and $\gamma_{c1} = c/l$ represent the geometric length scale ratio and contact length scale ratio at the microscale within a cluster, respectively (see Fig. 2b). For a mixed chain of a length $L_t(\lambda)$, the number of particles for each chain is $L_t(\lambda)/a$; thus, the resistance of each chain can be obtained as

$$R_c = \frac{L_t(\lambda)}{a}R_1 = \frac{L_t(\lambda)}{\lambda^2}\left[\frac{\gamma_{a1}/\gamma'_{a1}}{k_s\gamma'_{a1} + 2k_f(1-\gamma'_{a1})} + \frac{1-\gamma_{a1}}{k_s\gamma_{c1}^2\gamma_{a1}'^2/\gamma_{a1}^2 + k_f\left(1-\gamma_{c1}^2\gamma_{a1}'^2/\gamma_{a1}^2\right)}\right] \tag{13}$$

To obtain the value of $\gamma'_{a1}(=a/\lambda)$ in Eqs. (12) and (13), we refer to Fig. 4a, which is a simplified cross section of a mixed chain of particle. Note that the microporosity within a cluster ϕ_c is given by

$$\phi_c = (\lambda^2 - a^2)/\lambda^2 = 1 - (a/\lambda)^2 \tag{14a}$$

Solving this equation for $\gamma'_{a1}(=a/\lambda)$, we have

$$\gamma'_{a1} = a/\lambda = \sqrt{1-\phi_c} \tag{14b}$$

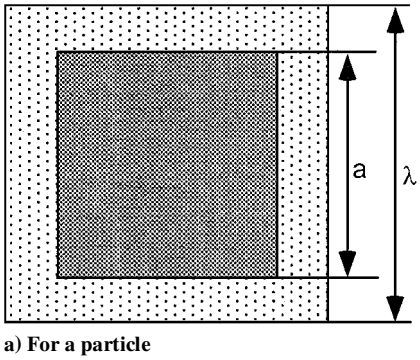

a) For a particle

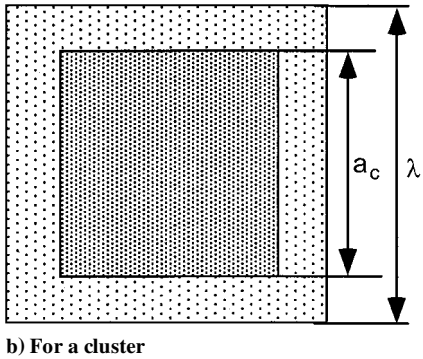

b) For a cluster

Fig. 4 Schematic of cross section of the mixed chains: ▨, fluid; ▩, particle; and ▥, cluster.

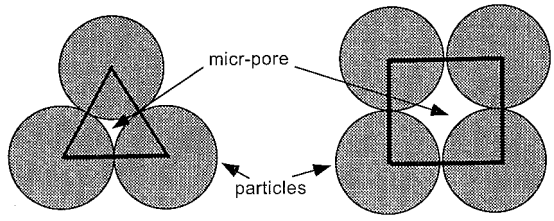

a) Triangular model **b) Square model**

Fig. 5 Possible configurations of particles.

The values of microporosity within a cluster ϕ_c depends on how the particles are packed. Figures 5a and 5b show two possible configurations of particles in a cluster. The porosities for the two configurations of particles are $\phi_c = 1 - \pi/2\sqrt{3}$ and $1 - \pi/4$, respectively, that is, $0.09 < \phi_c < 0.2$ in a cluster.

In the interval λ and $\lambda + \mathrm{d}\lambda$, there are the parallel chains of $(-\mathrm{d}N)$ that satisfy Eq. (8). Their resistance is $(-\mathrm{d}N/R_c)$, and the total resistance of the mixed chains in a unit cell is

$$\frac{1}{R_{\mathrm{mc}}} = -\int \frac{\mathrm{d}N}{R_c} \tag{15}$$

Inserting Eqs. (6), (8), and (14) into Eqs. (13) and (15), we obtain the dimensionless effective thermal conductivity of the parallel chains in a unit cell:

$$k^+_{e,\mathrm{mc}} = \frac{k_{e,\mathrm{mc}}}{k_f} = \frac{L_0}{A}\frac{1}{k_f R_{\mathrm{mc}}} = \frac{\lambda_{\max}^2}{A}\left(\frac{\lambda_{\max}}{L_0}\right)^{D_T-1}\frac{D_f}{1+D_T-D_f} \times \left\{1\Big/\left[\frac{\gamma_{a1}/\sqrt{1-\phi_c}}{\beta\sqrt{1-\phi_c}+2\left(1-\sqrt{1-\phi_c}\right)} + \frac{1-\gamma_{a1}}{\gamma_{c1}^2(1-\phi_c)(\beta-1)/\gamma_{a1}^2+1}\right]\right\} \tag{16}$$

where $\lambda_{\max}^2/A$ is the ratio of the maximum area of cross section of a mixed chain to the representative area A and $\lambda_{\max}/L_0$ is the ratio of the maximum diameter of cross section of a mixed chain to the representative length L_0 along the heat flow direction. The integration of Eq. (15) is performed over the entire range of chain sizes from $\lambda_{\min} = 0$ to $\lambda_{\max}$ under the assumption of $\lambda_{\min} \ll \lambda_{\max}$. To obtain the analytical expression, we take the averaged $\gamma'_{a1}[=\sqrt{(1-\phi_c)}]$ in the preceding integration. Combining Eqs. (10), (11), and (16), we have the fractal effective thermal conductivity expression for a cluster in the dimensionless form as

$$k^+_{e,c} = \frac{A_n}{A}k^+_{e,n} + \left(1-\frac{A_n}{A}\right)k^+_{e,\mathrm{mc}} = \frac{A_n}{A}\frac{k_{e,n}}{k_f} + \left(1-\frac{A_n}{A}\right)\frac{k_{e,\mathrm{mc}}}{k_f}$$
$$= \frac{A_n}{A}\left[\left(1-\sqrt{1-\phi_c}\right) + \frac{\sqrt{1-\phi_c}}{1+(1/\beta-1)\sqrt{1-\phi_c}}\right] + \left(1-\frac{A_n}{A}\right)\frac{\lambda_{\max}^2}{A}\left(\frac{\lambda_{\max}}{L_0}\right)^{D_T-1}\frac{D_f}{1+D_T-D_f} \times \left\{1\Big/\left[\frac{\gamma_{a1}/\sqrt{1-\phi_c}}{\beta\sqrt{1-\phi_c}+2\left(1-\sqrt{1-\phi_c}\right)} + \frac{1-\gamma_{a1}}{\gamma_{c1}^2(1-\phi_c)(\beta-1)/\gamma_{a1}^2+1}\right]\right\} \tag{17}$$

where ϕ_c is the porosity in a cluster and is given by Eq. (4).

When a similar method is applied, the effective thermal conductivity of bidispersed porous media can be obtained by

$$k_e^+ = \frac{A_n}{A}\left[\left(1-\sqrt{1-\phi}\right)+\frac{\sqrt{1-\phi}}{1+\left(1/k_{e,c}^+-1\right)\sqrt{1-\phi}}\right] + \left(1-\frac{A_n}{A}\right)\frac{\lambda_{\max}^2}{A}\left(\frac{\lambda_{\max}}{L_0}\right)^{D_T-1}\frac{D_f}{1+D_T-D_f} \times\left\{1\Big/\left[\frac{\gamma_a/\gamma_a'}{k_{e,c}^+\gamma_a'+2(1-\gamma_a')}+\frac{(1-\gamma_a)}{\gamma_c^2\gamma_a'^2\left(k_{e,c}^+-1\right)/\gamma_a^2+1}\right]\right\} \tag{18}$$

where $\gamma_a = l_c/a_c$ and $\gamma_c = c_c/l_c$ are the geometric length scale ratio and contact length scale ratio at the macroscale for clusters in a bidispersed medium, respectively (see Fig. 2a). Because of the statistically self-similarity existing in the micro- and macrostructures, the same values of $\lambda_{\max}^2/A$, $\lambda_{\max}/L_0$, D_T, and D_f used in Eqs. (17) and (18) are assumed in this model. In Eq. (18), γ_a' is given by

$$\gamma_a' = a_c/\lambda = \sqrt{(1-\phi)/(1-\phi_c)} \tag{19a}$$

According to Fig. 4b, the averaged porosity of a bidispersed medium is given by

$$\phi = \left[\left(\lambda^2 - a_c^2\right) + a_c^2\phi_c\right]/\lambda^2 \tag{19b}$$

In this model, we assume that the fractal dimension D_f of the area of cross section of the mixed chains is the same as the solid (or cluster) area fractal dimension, which can be estimated by the box-counting method.[15]

The algorithm for the determination of the thermal conductivity of a bidispersed porous medium is summarized as follows:

1) Given a porosity ϕ and the ratio of ϕ_c/ϕ, we can find the microporosity ϕ_c in clusters and obtain the fractal dimension D_f and D_T from the box-counting method.

2) Estimate the value of γ_{c1} and find γ_{a1} from Eq. (4).

3) Estimate the value of γ_c and find γ_a from Eq. (3).

4) The values of γ_{a1}' and γ_a' are computed from Eqs. (14) and (19), respectively.

5) The value of β can be computed if thermal conductivities of the solid and fluid phases are known.

6) Estimate the values of A_n/A, $\lambda_{\max}^2/A$, and $\lambda_{\max}/L_0$, and find the thermal conductivity $k_{e,c}^+$ of a cluster from Eq. (17).

7) Find the thermal conductivity for a bidispersed porous medium from Eq. (18).

Because the microstructure of a bidispersed porous medium is very complex, the ratios A_n/A, $\lambda_{\max}^2/A$, $\lambda_{\max}/L_0$, γ_{c1}, and γ_c can not be determined analytically, and they can only be determined experimentally. Once these values have been determined, the proposed fractal thermal conductivity model can be used to find the thermal conductivity of a bidispersed porous medium.

In this model, $D_f = 2$ corresponds to the situation in which a cross section is totally occupied by the mixed chains, and the effect of nontouching particles (or clusters) on the thermal conductivity is negligible, which will result in the very high thermal conductivity. However, note that in this model $D_f = 2$ does not imply that the solid volume fraction of the medium is 1 because the solid volume fraction of each chain is not unity, although the cross section is totally occupied by the mixed chains as $D_f = 2$, as shown in Fig. 6a. This means that, as $D_f = 2$, the porosity of a medium can be any value of $0 \le \phi \le 1$. Figure 6b shows that $D_f < 2$ as a cross section is not totally occupied by the mixed chains, and it is clearly shown that the porosity of the medium in this case is also less than 1. If and only if the porosity is equal to zero or the solid volume fraction is 1, the thermal conductivity can reach the maximum value (as $\beta > 1$). However, there is no quantitative relationship between the fractal dimension D_f and the solid volume fraction V_s in this model. In the next section we present a simplified model, in which a quantitative relationship between the fractal dimension and the solid volume fraction is presented.

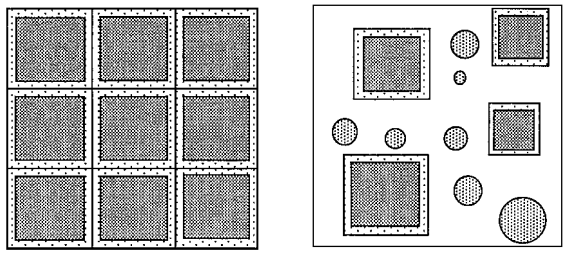

Fig. 6 Area fractal dimension and porosity for model 1: □, fluid; ■, solid; and ◍, non-touching particles or clusters.

Model 2: Simplified Model

In this simplified model, we assume that there is no fluid laterally enclosing the particle in the particle/cluster chains (see Figs. 4a and 4b) and that lateral contact resistance is neglected. This is equivalent to setting $\gamma_{a1}' = a/\lambda = 1$ in Eq. (14b) and $\gamma_a' = a_c/\lambda = 1$ in Eq. (18). Thus, Eqs. (17) and (18) become

$$k_{e,c}^+ = \frac{A_n}{A}\left[\left(1-\sqrt{1-\phi_c}\right)+\frac{\sqrt{1-\phi_c}}{1+(1/\beta-1)\sqrt{1-\phi_c}}\right] + \left(1-\frac{A_n}{A}\right)\frac{\lambda_{\max}^2}{A}\left(\frac{\lambda_{\max}}{L_0}\right)^{D_T-1}\frac{D_f}{1+D_T-D_f} \times\left\{1\Big/\left[\frac{\gamma_{a1}}{\beta}+\frac{(1-\gamma_{a1})}{\gamma_{c1}^2(\beta-1)/\gamma_{a1}^2+1}\right]\right\} \tag{20}$$

$$k_e^+ = \frac{A_n}{A}\left[\left(1-\sqrt{1-\phi}\right)+\frac{\sqrt{1-\phi}}{1+\left(1/k_{e,c}^+-1\right)\sqrt{1-\phi}}\right] + \left(1-\frac{A_n}{A}\right)\frac{\lambda_{\max}^2}{A}\left(\frac{\lambda_{\max}}{L_0}\right)^{D_T-1}\frac{D_f}{1+D_T-D_f} \times\left\{1\Big/\left[\frac{\gamma_a}{k_{e,c}^+}+\frac{(1-\gamma_a)}{\gamma_c^2\left(k_{e,c}^+-1\right)/\gamma_a^2+1}\right]\right\} \tag{21}$$

respectively. Because the fluid lateral to the chains is not included in the solid (particle or cluster) chains in this model, it is possible to find the quantitative relationship between the fractal dimension and the porosity (or solid volume fraction).

For the present bidispersed media, we can also choose the equilateral triangle unit cell (as shown in Figs. 7a and 7b), which has the effective porosity given by

$$\phi = \left[(A - \pi r^2/2) + \phi_c\pi r^2/2\right]/A \tag{22}$$

where A and r are the total area of the unit cell and radius of a cluster. Solving Eq. (22) for A gives

$$A = \tfrac{1}{2}\pi r^2[(1-\phi_c)/(1-\phi)] \tag{23a}$$

which can be written in the following dimensionless form:

$$A^+ = \tfrac{1}{2}d^{+2}[(1-\phi_c)/(1-\phi)] \tag{23b}$$

where $A^+ = A/(\pi d_0^2/4)$ and $d^+ = 2r/d_0$ with d_0 being the minimum diameter of a particle.

It is known that the Sierpinski gasket (as shown in Fig. 7c) is an exact self-similarity fractal geometry with the (shaded area) fractal dimension of $D_f = \ln 3/\ln 2 = 1.585$ $(3 = 2^{D_f})$ (Ref. 9). However, the Sierpinski gasket is only the special case $(L = 2)$ of Sierpinski-type gaskets.[20] Figures 7d–7f demonstrate the Sierpinski-type gaskets with $L = 3$, 5, and 6, respectively, and the shaded (solid) area fractal dimensions are $D_f = \ln 6/\ln 3 = 1.631$ $(6 = L^{D_f} = 3^{D_f})$, $D_f = \ln 12/\ln 5 = 1.544$ $(12 = L^{D_f} = 5^{D_f})$, and $D_f = \ln 15/\ln 6 = 1.511$ $(15 = L^{D_f} = 6^{D_f})$, respectively. The Sierpinski-type gaskets and their constructions

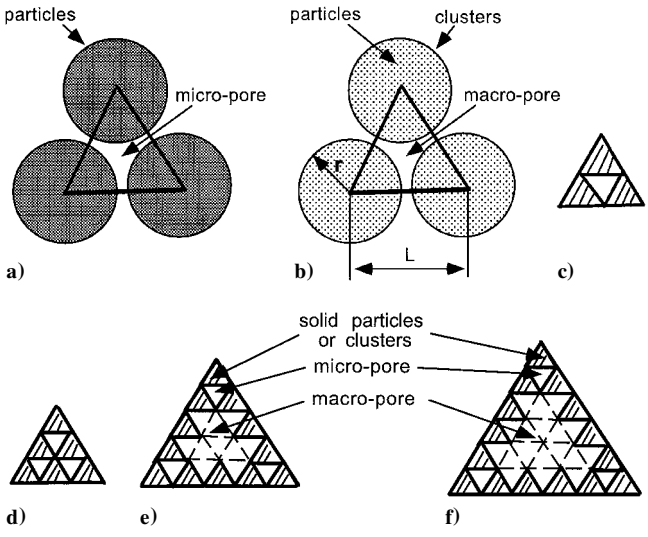

Fig. 7 Sierpinski gasket model for the bidispersed porous medium: a) microstructure of particles, b) macrostructure of clusters, c) Sierpinski gasket with $L = 2$, d) Sierpinski-type gasket with $L = 3$, e) Sierpinski-type gasket with $L = 5$, and f) Sierpinski-type gasket with $L = 6$.

are given by Yu and Yao.[20] In this paper, the Sierpinski-type gasket model is applied to simulate the present bidispersed porous media. However, this does not imply that there are quantitative relationships between the Sierpinski-type gaskets and the current bidispersed porous media for the thermal conductivity. Examining Figs. 7a–7f, we can find the approximate self-similarity existing in the macrostructure between clusters and the microstructure between particles inside clusters. This suggests that the Sierpinski-type gasket model can be used to simulate bidispersed porous media. Therefore, the total solid (shaded) area for the unit cell, as shown in Fig. 7b, can be approximately calculated by

$$A_s = (L^+)^{D_f} \tag{24}$$

where $L^+ = L/d_0$ and A_s is the dimensionless area. It follows from Eq. (24) that

$$D_f = \ln A_s \Big/ \ln L^+ \tag{25}$$

If the unit cell is covered with a dense or compact substance (such as solid cooper), the fractal dimension for the substance will be 2. For example, if Fig. 7e is completely covered with solid, its volume fraction is 1, and the solid area fractal dimension is 2 ($25 = 5^{D_f}$, and so $D_f = 2$). The solid volume fraction of the unit cell can be expressed as

$$V_s = A_s \Big/ A^+ = 1 - \phi \tag{26}$$

where the total area of the unit cell can be written as

$$A^+ = L^{+2} \tag{27}$$

or

$$L^+ = \sqrt{A^+} = d^+ \sqrt{(1 - \phi_c)/2V_s} \tag{28}$$

Combining Eqs. (25–28) yields

$$D_f = 2 + \frac{\ln V_s}{\ln\left[d^+ \sqrt{(1 - \phi_c)/2V_s}\right]} \tag{29}$$

Equation (29) reveals that the area fractal dimension is a function of microporosity, solid volume fraction, and the ratio of the averaged cluster size to the minimum particle size. Equation (29) shows that $D_f = 2$ for $V_s = 1$ and vice versa. This is consistent with the physical situation. If we set $\phi_c = 0$, Eq. (29) can be reduced to

$$D_f = 2 + \frac{\ln V_s}{\ln\left(d^+ \sqrt{1/2V_s}\right)} \tag{30}$$

which can be used to describe the fractal dimension of a monodispersed porous medium.

V. Results and Discussion

It may be recalled that the present fractal thermal conductivity models are based on the fundamental relationship between the number of cumulative cross sections of mixed chains and area sizes, given by Eq. (7). The existence of the scaling relationship in actual microstructures is shown in Fig. 8, which was obtained by the box-counting method.[15] Figure 8 shows a log–log plot of the cumulative number of areas of solid, $N(L \geq \lambda) \sim \lambda$. The fractal dimensions, $D_f = 1.74$ and 1.73, are obtained by the box-counting method for the bidispersed porous media with the porosity of 0.52 and 54, respectively. It is seen that the number of cumulative areas of cross section of the mixed chains decreases as the chain size λ increases. The data follow a linear relationship on the logarithmic scale, which confirms the statistical fractal nature of the microstructures of the bidispersed porous media. Note that, although the Sierpinski gasket model is applied to establish the relationship between the fractal dimension and solid volume fraction of the bidispersed porous medium in this paper, it cannot be applied to obtain the thermal conductivity of the bidispersed porous media.

Figure 9 shows that when the relative cluster size $d^+ = 18$, the best fit to the data from the box-counting method is obtained. With the value of $d^+ = 24$, the relative errors between the box-counting method and the theoretical predictions from Eq. (29) are about 1%. This means that the ratio of the minimum particle size to the maximum cluster size is about 4–5%. Figure 9 also indicates that the smaller the relative cluster size d^+ is, the lower the fractal dimension. The reason is that, when the cluster becomes smaller at fixed solid volume fraction V_s, the total area A^+ also becomes smaller. This leads to the decrease of the total solid area A_s at fixed V_s and results in the decrease of the solid area fractal dimension. From Fig. 9, it can also be seen that the solid area fractal dimensions will approach its possible maximum value of 2 as the solid volume fraction reaches the value of 1. This is what is expected and is consistent with the actual physical situation, which verifies the present fractal dimension model.

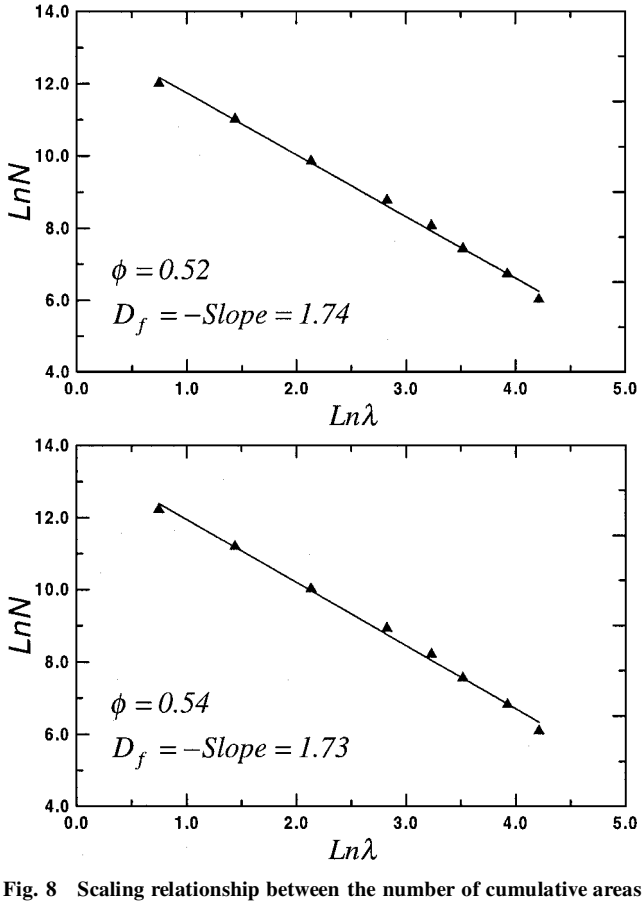

Fig. 8 Scaling relationship between the number of cumulative areas of cross section of chains and chain sizes from the box-counting method.

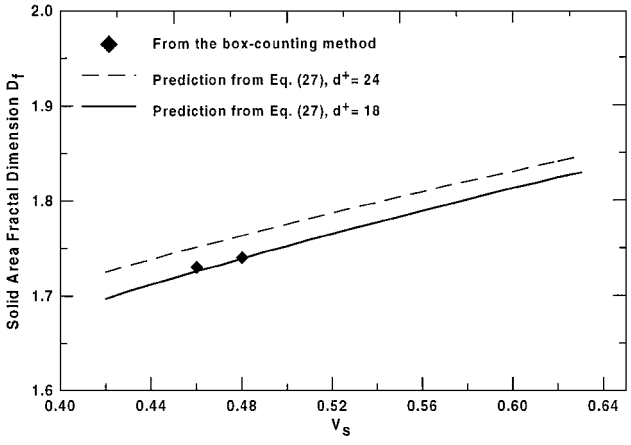

Fig. 9 Comparison of the fractal dimension vs the solid volume fraction and cluster size.

Figure 10 shows a comparison of the effects of the tortuosity dimension D_T, the area fractal dimension D_f, and the porosity on the predicted thermal conductivities based on the simplified model 2. Figure 10a shows the thermal conductivity variation with the tortuosity dimension D_T, at a fixed area dimension of $D_f = 1.74$ and a fixed porosity $\phi = 0.52$. It is seen that the thermal conductivity decreases as D_T increases. The decrease in thermal conductivity with the increase in D_T is attributed to the increased heat resistance due to the higher convoluted chains (the higher the tortuosity dimension, the higher the resistance). Figure 10b shows that the thermal conductivity increases with the fractal dimension D_f at fixed D_T and porosity. The reason is that an increase in D_f corresponds to the increase of area consisting of mixed chains [see also Eq. (5)], which results in the increase of the thermal conductivity. Figure 10c shows the effect of the porosity on the thermal conductivity at the fixed D_f and D_T. It is seen that the thermal conductivity increases as the porosity decreases. This can be interpreted as when the porosity decreases, the solid volume fraction increases, which leads to the increase of the thermal conductivity as $\beta > 1$. The opposite results exist as $\beta < 1$ (see Fig. 10c). This is exactly what is expected. Similar results hold for model 1.

Figure 11 shows a comparison of the existing experimental data[4,21] on the thermal conductivities of monodispersed porous media at a porosity of 0.38 ($V_s = 0.62$) with the predicted values based on the present fractal models 1 and 2 given, respectively, by Eqs. (17) and (20), with the parameters $D_f = 1.80$ (estimated from Fig. 9), $D_T = 1.2$, $A_n/A = 0.7$, $\lambda_{\max}/L_0 = 0.2$, $\gamma_{c1} = 0.13$ (same value as that used by Hsu et al.[6]), $\gamma_c = 0.13$ (estimated), and $\lambda^2_{\max}/A = 0.12$ for model 1 and $\lambda^2_{\max}/A = 0.10$ for model 2. The results from the Hsu et al. model[6] given by Eq. (2) for a monodispersed porous medium at $\phi = 0.38$ and $\gamma_{c1} = 0.13$ are also shown in Fig. 11 for comparison. It is seen that the thermal conductivities of a monodispersed porous medium predicted by the two fractal models are in good agreement with each other. For $10 < \beta < 5000$, the fractal models are slightly higher than the experimental data[4,21] and the Hsu et al. model,[6] and for $\beta < 1$, the predictions from the present fractal models are lower than those predicted by the Hsu et al. model as well as the experimental data.

Figure 12 is a comparison of the present fractal models 1 and 2 for bidispersed porous media at the porosity of 0.52, given by Eqs. (18) and (21), respectively. The Chen et al. model given by Eq. (1) and their experimental data[8] are also presented for comparison purposes. The computations were based on the values of $\phi_c/\phi = 0.342$, $\gamma_{c1} = 0.53$, and $\gamma_c = 0.37$ taken from Ref. 8, with the parameters $A_n/A = 0.7$, $\lambda_{\max}/L_0 = 0.2$, and $D_T = 1.12$. We used $\lambda^2_{\max}/A = 0.27$ for model 1 and $\lambda^2_{\max}/A = 0.20$ for model 2. From Fig. 12, it is seen that the predicted thermal conductivites of a bidispersed porous medium based on fractal models 1 and 2 are also in good agreement with those predicted from the Chen et al. model, as well as with their experimental data.[8] Because no other experimental data on the thermal conductivity of bidispersed porous media are available, only the Chen et al. data[8] for bidispersed porous media are presented for comparison. From Figs. 11 and 12, we can conclude that the thermal conductivities predicted by the two fractal models 1 and 2 are almost the same; thus, the assumption used for model 2 regarding no fluid laterally enclosing the particles is justified. This also implies that the lateral heat conductivity has little influence on total heat flow and, hence, also justifies the assumption that contact resistance is mainly along the heat flow direction and that heat conduction/contact resistance in the lateral direction is not significant.

Note that we used $\lambda^2_{\max}/A = 0.27$ for model 1, which is higher than that the value of 0.20 for model 2 at the porosity of 0.52. This is because the chains are coated with fluid in model 1, which makes the area of the cross section of each chain greater than that in model 2, in which the chains are not coated (or surrounded) by fluid. The same reason is applicable for the lower porosity of 0.38,

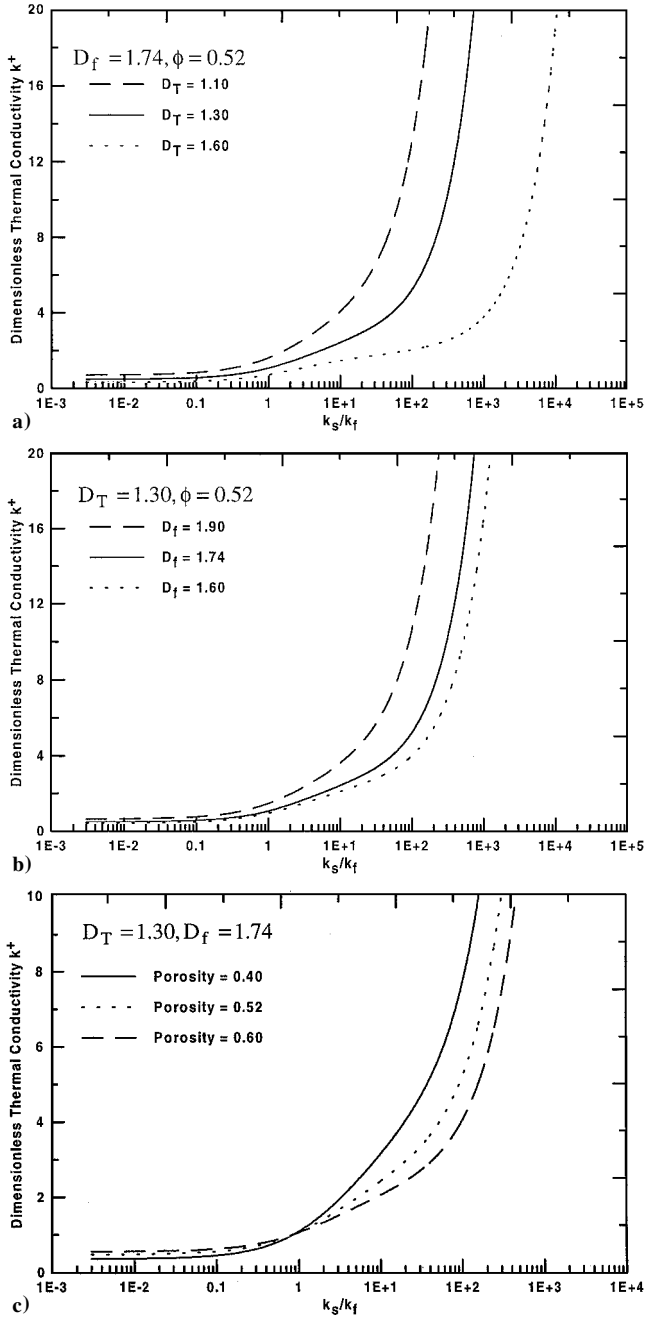

Fig. 10 Effect of parameters on the thermal conductivities: a) thermal conductivity vs the tortuosity fractal dimension at $D_f = 1.74$ and $\phi = 0.52$, b) thermal conductivity vs the area fractal dimension at $D_T = 1.30$ and $\phi = 0.52$, and c) thermal conductivity vs the porosity at $D_T = 1.30$ and $D_f = 1.74$.

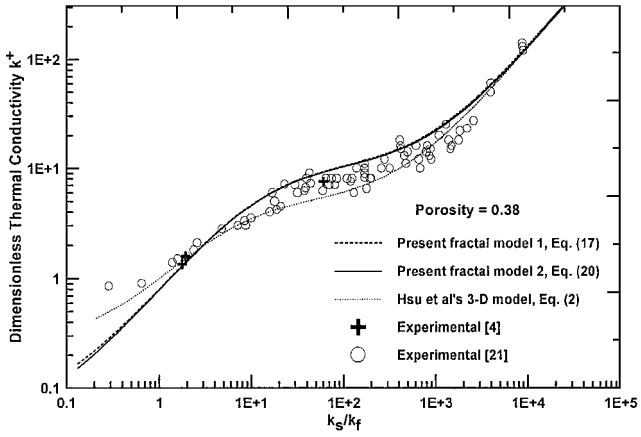

Fig. 11 Comparison among the Hsu et al. model, present fractal models 1 and 2 ($D_f = 1.80$), and other investigators' experimental data for monodispersed porous media.

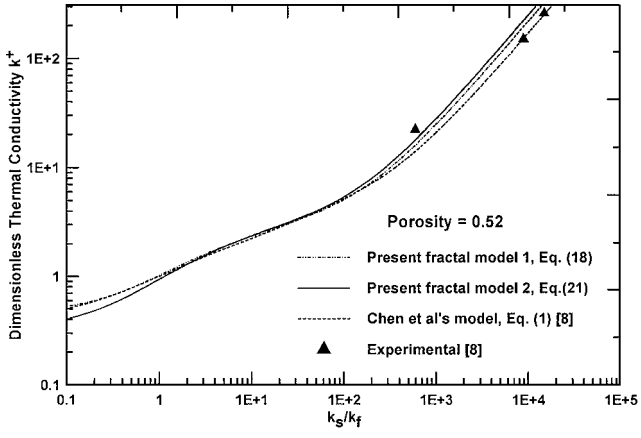

Fig. 12 Comparison among the present fractal models 1 and 2 ($D_f = 1.74$), the Chen et al. model,[8] and experimental data[8] for bidispersed porous media.

for which $\lambda_{\max}^2/A = 0.12$ and $\lambda_{\max}^2/A = 0.10$ are used for models 1 and 2, respectively. Theoretically, the tortuosity fractal dimension D_T can be also determined by the box-counting method similar to those of obtaining the area fractal dimension D_f. However, because the clusters in the samples contained very small copper particles that disappeared after polishing, the tortuosity fractal dimension D_T of the structures of samples cannot be measured by the box-counting method, and only estimated value of D_T was provided.

Finally, note the differences between the present fractal model and the Chen et al. model[8] given by Eqs. (1) and (2). In the Chen et al. model, particles or clusters of uniform size with a periodic structure and three-dimensional contact resistances are assumed. In the present fractal model, the particles or clusters are not of the same size, and one-dimensional contact resistance is assumed to be along the heat flow direction only. Although the current fractal model and the lumped-parameter model given by Eqs. (1–4) give almost the same satisfactory results compared with the experimental data, the present fractal model is more realistic for the random or disordered media. This is because porous media consisting of uniform particles or clusters with a periodic structure are rarely found in nature. This paper presents a preliminary fractal analysis of the effective thermal conductivity for bidispersed porous media. However, estimation of the parameters such as the ratios A_n/A, $\lambda_{\max}^2/A$, and $\lambda_{\max}/L_0$ is not an easy task.

VI. Conclusions

Two fractal thermal conductivity models are derived based on the fractal characteristics of the microstructures of bidispersed porous media and on the electrical analogy technique. The proposed fractal thermal conductivity models are a function of the tortuosity fractal dimension, area fractal dimension, porosity, and ratios of areas, length scale, and contact length. The two fractal models are separately compared with both the lumped-parameter model and experimental data, and good agreement is found among them. The fractal models may be particularly useful for the random porous media with nonuniform particles or clusters.

Note that we have assumed one-dimensional heat conduction in the unit cell, and the heat flow lines approximately follow the chains for simplicity purposes in this paper. In reality, the lateral heat conduction, that is, two-dimensional heat conduction, should be considered for a better modeling. This aspect of the problem will be considered in our future work.

Acknowledgment

This work was supported by the Research Grant Council of the Hong Kong Special Administrative Region through Grant HKUST6044/97E.

References

[1]Behrens, E., "Thermal Conductivities of Composite Materials," *Journal of Composite Materials*, Vol. 2, No. 1, 1968, pp. 2–17.

[2]Han, L. S., and Cosner, A. A., "Effective Thermal Conductivities of Fibrous Composites," *Journal of Heat Transfer*, Vol. 103, May 1981, pp. 387–392.

[3]Hadley, G. R., "Thermal Conductivity of Packed Metal Powers," *International Journal of Heat and Mass Transfer*, Vol. 29, No. 5, 1986, pp. 909–920.

[4]Prasad, V., Kladias, N., Bandyopadhaya, A., and Tian, Q., "Evaluation of Correlations for Stagnant Thermal Conductivity of Liquid-Saturated Porous Beds of Spheres," *International Journal of Heat and Mass Transfer*, Vol. 32, No. 9, 1989, pp.1793–1796.

[5]Verma, L. S., Shrotriya, A. K., Ramvir, S., and Chaudhary, D. R., "Thermal Conduction in Two-Phase Materials with Spherical and Non-Spherical Inclusions," *Journal of Physics D: Applied Physics*, Vol. 24, No. 10, 1991, pp. 1729–1737.

[6]Hsu, C. T., Cheng, P., and Wong, K. W., "A Lumped-Parameter Model for Stagnant Thermal Conductivity of Spatially Periodic Porous Media," *Journal of Heat Transfer*, Vol. 117, May 1995, pp. 264–269.

[7]Cheng, P., and Hsu, C. T., "The Effective Stagnant Thermal Conductivity of Porous Media with Periodic Structures," *Journal of Porous Media*, Vol. 2, No. 1, 1999, pp. 19–38.

[8]Chen, Z. Q., Cheng, P., and Hsu, C. T., "Effective Thermal Conductivity of Bi-Dispersed Porous Media," *Proceedings of Symposium on Energy Engineering in the 21st Century*, Vol. 2, edited by P. Cheng, Begell House, New York, 2000, pp. 505–511.

[9]Mandelbrot, B. B., *The Fractal Geometry of Nature*, W. H. Freeman, New York, 1982, pp. 23–57.

[10]Feder, J., *Fractals*, Plenum, New York, 1988, pp. 8–14.

[11]Warren, T. L., and Krajcinovic, D., "Random Cantor Set Models for the Elastic–Perfectly Plastic Contact of Roughness Surfaces," *Wear*, Vol. 196, 1996, pp. 1–15.

[12]Majumdar, A., and Bhushan, B., "Role of Fractal Geometry in Roughness Characterization and Contact Mechanics of Surfaces," *Journal of Tribology*, Vol. 112, April 1990, pp. 205–216.

[13]Katz, A. J., and Thompson, A. H., "Fractal Sandstone Pores: Implications for Conductivity and Pore Formation," *Physical Review Letters*, Vol. 54, No. 12, 1985, pp. 1325–1328.

[14]Sreenivasan, K. R., "Fractals and Multifractals in Fluid Turbulence," *Annual Review of Fluid Mechanics*, 1991, pp. 539–600.

[15]Yu, B., and Cheng, P., "A Fractal Permeability Model for Bi-Dispersed Porous Media" (submitted for publication).

[16]Wheatcraft, S. W., and Tyler, S. W., "An Explanation of Scale-Dependent Dispersivity in Heterogeneous Aquifers Using Concepts of Fractal Geometry," *Water Resources Research*, Vol. 24, No. 4, 1988, pp. 566–578.

[17]Sahimi, M., *Flow and Transport in Porous Media and Fractured Rocks*, VCH Verlagsgesellshaft, Weinheim, Germany, 1995, p. 13.

[18]Vicsek, T., *Fractal Growth Phenomena*, World Scientific, Singapore, 1989, p. 15.

[19]Majumdar, A., "Role of Fractal Geometry in the Study of Thermal Phenomena," *Annual Review of Heat Transfer*, Vol. 4, edited by C. L. Tien, Hemisphere, New York, 1992, pp. 56, 57.

[20]Yu, B.-M., and Yao, K.-L., "Numerical Evidence of the Critical Percolation Probability for Site Problems on Sierpinski Gaskets," *Journal of Physics A: General Physics*, Vol. 21, 1988, pp. 3269–3274.

[21]Kaviany, M., *Principles of Heat Transfer in Porous Media*, Springer-Verlag, New York, 1995, p. 147.